

EPISODIC JETS AS THE CENTRAL ENGINE OF GAMMA-RAY BURSTS

FENG YUAN¹ AND BING ZHANG²

Draft version January 15, 2021

ABSTRACT

Most Gamma-ray bursts (GRBs) have erratic light curves, which demand that the GRB central engine launches an episodic outflow. Recent Fermi observations of some GRBs indicate a lack of the thermal photosphere component as predicted by the baryonic fireball model, which suggests a magnetic origin of GRBs. In view that powerful episodic jets have been observed along with continuous jets in other astrophysical black hole systems, here we propose an intrinsically episodic, magnetically-dominated jet model for GRB central engine. Accumulation and eruption of free magnetic energy in the corona of a differentially-rotating, turbulent accretion flow around a hyperaccreting black hole lead to ejections of episodic, magnetically dominated plasma blobs. These blobs are accelerated magnetically, collide with each other at large radii, trigger rapid magnetic reconnection and turbulence, efficient particle acceleration and radiation, and power the observed episodic prompt gamma-ray emission from GRBs.

Subject headings: accretion, accretion disks – gamma-rays burst: general – magnetic reconnection – ISM: jets and outflows

1. INTRODUCTION

Observations of gamma-ray bursts (GRBs) suggest that the GRB central engine is able to launch an ultra-luminous, highly relativistic jet. Most GRBs have erratic, rapidly varying lightcurves (Fishman & Meegan 1995), typically lasting 10s to 100s of seconds for long-duration GRBs, and less than 2 seconds for short-duration GRBs. Recent observations of GRBs pose some important constraints on the models of GRB central engine. First, recent Fermi Large Area Telescope (LAT) observations suggest that most GRBs have featureless smoothly joint broken power-law spectra (i.e. Band-function spectra (Band et al. 1993)) in a wide energy band (Abdo et al. 2009; Zhang et al. 2011). The standard fireball model predicts a strong thermal emission component from the fireball photosphere (Paczynski 1986; Mészáros & Rees 2000; Pe'er 2006). The non-detection likely suggests that the GRB outflow is magnetically dominated (Zhang & Pe'er 2009; Fan 2010). Second, data analysis suggests that the GRB lightcurves not only can be decomposed into many pulses (Norris et al. 1996; Hakkila et al. 2003), but most of them can be also decomposed into the superposition of a fast, spiky component and a slow, smooth component (Gao, Zhang, & Zhang 2012; Vetere et al. 2006). A radiation model that invokes magnetic turbulent reconnection triggered by collisions of magnetically-dominated blobs has been proposed (Zhang & Yan 2011), which can interpret the new observational data. This radiation model requires a central engine that can eject an episodic, magnetically dominated jet.

The leading model of GRB central engine invokes a hyperaccreting black hole (Narayan et al. 1992; Mészáros et al. 1999; Narayan et al. 2001). In most previous GRB central engine models, the rapid variability in the erratic light curves is attributed either to the intermittency of the accretion flow, i.e. a time-dependent accretion rate \dot{M} (MacFadyen & Woosley 1999), or to the instability during the propagation of the jet in the stellar envelope (Zhang et al. 2003; Morsony et al.

2010). For a magnetically dominated central engine, the leading model is the Blandford-Znajek (BZ) mechanism (Blandford & Znajek 1977), which requires a large-scale open magnetic field connecting the black hole and an external astrophysical load, whose origin is an open question. This model also tends to generate a continuous jet, unless the accretion rate is highly variable. Screw or kink instabilities (Li 2000; Mizuno et al. 2009) are invoked to disrupt a continuous jet and produce discrete blobs. Since the BZ mechanism is powered by accretion, the immediate advantage of involving BH spin rather than accretion disk as the source of jet power is not evident.

On the other hand, in addition to the continuous jets, episodic jets, which is intermittent and in the form of discrete moving blobs, have been observed in other black hole systems. A magnetohydrodynamical model has been proposed to explain the formation of these episodic jets (Yuan et al. 2009). In this paper, we propose a central engine model for GRBs, based on this idea. A review on observations and the model of episodic jets are presented in Section 2. Our model is delineated in detail in Section 3. The salient features of the model are summarized in Section 4.

2. EPISODIC JETS IN BLACK HOLE SYSTEMS AND THEIR FORMATION MECHANISM

Episodic jets are most evidently observed in black hole X-ray binaries, e.g., in GRS 1915+105 and GRO J1655-40 (Mirabel & Rodriguez 1994; Hjellming & Rupen 1995; Fender & Belloni 2004), and also in AGNs, as manifested as knots or blobs, e.g., in 3C 120 (Marscher et al. 2002; Chatterjee et al. 2009) and NGC 4258 (Doi et al. 2011). In the case of 3C 120, knots have been directly resolved as due to episodic ejections and their ejection times have been determined by extensive radio monitoring observations. In the case of the supermassive black hole in our Galactic center, we have strong evidence for episodic jets, but no continuous jets have ever been detected (Yuan 2011). The differences of the properties of the two types of jets are summarized in Fender & Belloni (2004). Among other things, episodic jets are much faster and more powerful. The collision between blobs is often invoked to explain the flares detected in AGN

¹ Shanghai Astronomical Observatory, Chinese Academy of Sciences, 80 Nandan Road, Shanghai 200030, China; fyuan@shao.ac.cn

² Department of Physics and Astronomy, University of Nevada Las Vegas, Las Vegas, NV 89154, USA; zhang@physics.unlv.edu

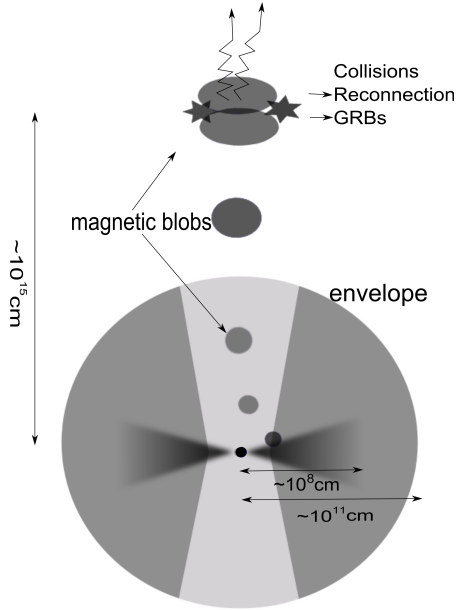


FIG. 1.— A cartoon picture of the episodic jet model. The typical distances are marked.

jets.

Yuan et al. (2009) proposed a magnetohydrodynamical model for the formation of episodic jets, by analogy of coronal mass ejection (CME) in the Sun. The basic scenario is the following. Closed magnetic field lines continuously emerge out of the accretion flow into the corona. Because of shear and turbulent motion of the accretion flow, the field line is twisted and deformed, resulting in formation of a flux rope in the corona. The flux rope is initially in force balance between magnetic tension and magnetic compression forces. Energy and helicity are accumulated and stored until a threshold is reached. The system then loses its equilibrium and the flux rope is thrust outward by the magnetic compression force in a catastrophic way, which causes an episodic jet. After a magnetic blob is ejected, the magnetic tension is temporarily relaxed. Later magnetic field emergence and distortion restart, and the above delineated process repeats. Within this scenario, no large-scale open magnetic field lines are needed. The basic picture has gained supports from some numerical simulations (e.g., Romanova 1998; Kudoh, Matsumoto & Shibata 2002; Machida, Nakamura, & Matsumoto 2004).

Within the GRB context, several magnetic central engine models have been proposed along the similar line. In the context of their neutron star central engine model, Blackman et al. (1996) pointed out that magnetically dominated blobs rather than a continuous jet have the advantage in reproducing the time structure of GRBs. Kluzniak & Ruderman (1998) and Dai & Lu (1998) also emphasized the importance of accumulation of magnetic fields and subsequent emergence to account for an episodic jet. A similar idea was proposed to interpret X-ray flares (Dai et al. 2006) in some short GRBs. Uzdensky & MacFadyen (2006, 2007) proposed a magnetic tower model for GRBs, which invokes extraction of the rotational energy of an accretion disk by amplification of the toroidal magnetic field (Lynden-Bell 1996). The model is essentially time-independent, different from the model discussed in Yuan et al. (2009) and below.

3. EPISODIC MAGNETIC JETS IN GRBS

We now extend the Yuan et al. (2009) scenario to GRBs. Our model can be sketched by Figure 1. We consider a stellar-size black hole surrounded by a hyperaccretion accretion flow with a typical accretion rate $\dot{M} \sim 0.1 M_{\odot} \text{s}^{-1}$. Neutrino cooling is important at $\lesssim 200GM/c^2$ (neutrino-dominated accretion flow: NDAF); outside of this radius the accretion flow is advection dominated Chen & Beloborodov (2007) (ADAF). The solutions for NDAF and ADAF can be described as (Narayan et al. 2001; Beloborodov 2003):

$$\rho = 6 \times 10^{13} \dot{M}_{32} \alpha_{-2}^{-1.3} M_3^{-1.7} r^{-2.55} \text{g cm}^{-3}, \quad (1)$$

$$T_c = 3 \times 10^{10} \alpha_{-2}^{0.2} M_3^{-0.2} r^{-0.3} \text{K}, \quad (2)$$

$$v_k = 2 \times 10^{10} r^{-0.5} \text{cm s}^{-1}, \quad (3)$$

$$v_r = 2 \times 10^6 \alpha_{-2}^{1.2} M_3^{-0.2} r^{0.2} \text{cm s}^{-1}, \quad (4)$$

and

$$\rho = 3 \times 10^{11} \alpha_{-2}^{-1} \dot{M}_{32} M_3^{-2} r^{-1.5} \text{g cm}^{-3}, \quad (5)$$

$$T_c = 3 \times 10^{11} \alpha_{-2}^{-1/4} \dot{M}_{32}^{1/4} M_3^{-0.5} r^{-5/8} \text{K}, \quad (6)$$

$$v_k = 2 \times 10^{10} r^{-0.5} \text{cm s}^{-1}, \quad (7)$$

$$v_r = \frac{\alpha}{\sqrt{5}} R \Omega_k = 10^8 \alpha_{-2} r^{-0.5} \text{cm s}^{-1}, \quad (8)$$

respectively. Here ρ is the density, T_c is the temperature at the equatorial plane, $v_k = \sqrt{GM/R}$ and v_r are the Keplerian and radial velocities, $\alpha = 0.01 \alpha_{-2}$ is the viscous parameter, r is radius R in unit of $2GM/c^2$, \dot{M}_{32} is the mass accretion rate in unit of 10^{32}g s^{-1} , and M_3 is the black hole mass in unit of $3 M_{\odot}$. The viscous timescales of the inner NDAF and outer ADAF are then

$$t_{\text{vis,NDAF}} = R/v_r = 17 \alpha_{-2}^{-1.2} M_3^{1.2} (r/100)^{0.8} \text{s}, \quad (9)$$

and

$$t_{\text{vis,ADAF}} = R/v_r = 30 \alpha_{-2}^{-1} M_3 (r/200)^{1.5} \text{s}, \quad (10)$$

respectively. Hereafter we normalize the NDAF solutions at $r = 100$ where the disk solution transits from NDAF to ADAF. All our ADAF solutions are normalized to $r = 200$, which corresponds to a viscous time scale ~ 30 s, the typical duration of a long GRB. We will show below that powerful episodic jets are launched in the ADAF regions, i.e. at radii larger than $r \sim 100$, since the ejection power of magnetic blobs is relatively suppressed in the NDAF region (see discussions below Eqs.(20,21)).

Now we estimate the energetics and time intervals of the magnetic blobs. The region where a magnetic blob occurs, i.e. the flux rope region in the disk corona, is special because the available free magnetic energy is large due to the topological structure of the magnetic field. By analogy with the CME theory of solar physics, the total available free magnetic energy of one blob is (Lin et al. 1998):

$$E_{\text{free}} \approx 0.5 \times \left(\frac{1}{12} B_0^2 V \right). \quad (11)$$

Here B_0 is the magnetic strength in the accretion disk, $V \sim \pi R^3$ is the volume of the system. Defining $\beta = P_{\text{mag}}/P_{\text{tot}}$, where $P_{\text{tot}} = (P_{\text{gas}} + P_{\text{rad}} + P_{\text{mag}} + P_{\nu}) \sim P_{\text{gas}}$ in NDAF and $P_{\text{tot}} = (P_{\text{gas}} + P_{\text{rad}} + P_{\text{mag}}) \sim P_{\text{rad}}$ in ADAF (where $P_{\text{mag}} (\equiv B^2/8\pi)$, P_{gas} , P_{rad} , P_{ν} and P_{tot} are magnetic, gas, radiation, neutrino, and total pressure in the accretion disk, respectively), one can

estimate the strength of magnetic field B_0 for a given β . Numerical simulations show that if the α viscosity is intrinsically the magnetic stress associated with the MHD turbulence driven by the magnetorotational instability (Balbus & Hawley 1991, 1998), as widely accepted, the values of α and β are not independent (Blackman et al. 2008). This is confirmed by recent numerical simulations (Hawley, Guan, & Krolik 2011; Sorathia et al. 2012). Noticing the different definitions between our work and Blackman et al. (2008), one should roughly have $\alpha/\beta \sim 0.1$ according to Blackman et al. (2008). Therefore $\alpha = 0.01$ implies that the value of β should be $\beta = 0.1\beta_{-1} = 0.1$. In the following we adopt $\alpha = 0.01$ and $\beta = 0.1$ as typical values. We note, however, that a much higher $\beta \gg 1$ can be achieved if the accretion material is already moderately magnetized at the beginning of accretion (Shibata, Tajima, & Matsumoto 1990; Johansen & Levin 2008).

For the inner gas-pressure-dominated NDAF and outer radiation-pressure-dominated ADAF, one has

$$\frac{B_0^2}{8\pi} \approx 0.1\beta_{-1}P_{\text{gas}}, \quad (12)$$

and

$$\frac{B_0^2}{8\pi} \approx 0.1\beta_{-1}P_{\text{rad}} = 0.1\beta_{-1} \frac{4\sigma}{3c} T_c^4, \quad (13)$$

respectively, so that the available energy in the NDAF and ADAF regions are

$$E_{\text{free,NDAF}} = 7.4 \times 10^{48} \alpha_{-2}^{-1.1} \beta_{-1} M_3^{1.1} \dot{M}_{32}(r/100)^{0.15} \text{erg}, \quad (14)$$

and

$$E_{\text{free,ADAF}} = 8.2 \times 10^{49} \alpha_{-2}^{-1} \beta_{-1} M_3 \dot{M}_{32}(r/200)^{0.5} \text{erg}, \quad (15)$$

respectively.

The time interval between two consecutive ejections can be estimated as the timescale to accumulate and release E_{free} in the flux rope system in the corona of the accretion flow. The first timescale is the energy accumulation time. The magnetic energy of the flux rope system is converted from the rotational energy of the accretion flow by Alfvén waves propagating along the magnetic field lines (Yuan et al. 2009). The energy density of the rotational energy is $\sim \rho v_k^2$ and the energy conversion speed is the Alfvén speed $v_A \equiv B_0/\sqrt{4\pi\rho}$. The energy transfer rate by the magnetic field is then $\dot{E}_{\text{mag}} = \rho v_k^2 v_A R^2$. The corresponding energy transfer timescale in the NDAF and ADAF regimes are

$$t_{\text{tran,NDAF}} = 4.2 \times 10^{-3} \alpha_{-2}^{0.1} \beta_{-1}^{0.5} M_3^{0.9} (r/100)^{1.85} \text{s}, \quad (16)$$

and

$$t_{\text{tran,ADAF}} = 4.8 \times 10^{-1} \beta_{-1}^{0.5} M_3 (r/200)^{1.5} \text{s}, \quad (17)$$

respectively.

The second relevant timescale is the emergence timescale of the magnetic field line from the disk to the corona due to Parker instability (Horiuchi et al. 1998):

$$t_{\text{parker,NDAF}} \approx \frac{5H}{v_A} \approx 4\alpha_{-2}^{-0.1} \beta_{-1}^{-0.5} M_3^{1.1} (r/100)^{1.15} \text{s} \gg t_{\text{tran,NDAF}}, \quad (18)$$

and

$$t_{\text{parker,ADAF}} \approx \frac{5H}{v_A} \approx 3.4\beta_{-1}^{-0.5} M_3 (r/200)^{1.5} \text{s} \gg t_{\text{tran,ADAF}}, \quad (19)$$

respectively. The time interval between two consecutive ejections is thus $t_{\text{int}} = t_{\text{tran}} + t_{\text{parker}} \simeq t_{\text{parker}}$ for both NDAF and ADAF. The power output from these two regions is then

$$P_{\text{NDAF}} = 1.8 \times 10^{48} \alpha_{-2}^{-1} \beta_{-1}^{1.5} \dot{M}_{32}(r/100)^{-1} \text{erg s}^{-1}, \quad (20)$$

and

$$P_{\text{ADAF}} = 2.4 \times 10^{49} \alpha_{-2}^{-1} \beta_{-1}^{1.5} \dot{M}_{32}(r/200)^{-1} \text{erg s}^{-1}, \quad (21)$$

respectively. One can see that the power output increases significantly beyond the “transition region” ($r \sim 100-200$) from NDAF to ADAF. So the ADAF region is the main region for powerful magnetic blob injection³. From now on, we focus on the ADAF only, and neglect the subscript “ADAF” in the equations.

For long GRBs, the jet-corrected total energy is of the order of 10^{51} erg (Frail et al. 2001; Liang et al. 2008; Racusin et al. 2009). Since a GRB may be powered by multiple collisions among blobs, each blob would carry an energy of $\sim 10^{50}$ erg. For $r \sim 100-200$, our estimate of Eq. (15) matches this observational fact well. Comparing Eqs. (19) and (10), we find that $t_{\text{int}} < t_{\text{vis}}$. This suggests that the system has enough time to store magnetic energy and to eject multiple magnetic blobs before being accreted into the black hole.

Following Uzdensky & MacFadyen (2006, 2007), we assume that a magnetic jet can penetrate through the star and remain intact. For episodic jet, this is possible as long as the time interval between two consecutive blobs is shorter than the time for the funnel to close, which is ~ 10 s (Wang & Mészáros 2007). This condition is satisfied for our model. After escaping the star, the magnetic blob undergoes acceleration under its own magnetic pressure gradient (Tchekhovskoy et al. 2010). An impulsive magnetic blob can reach $\Gamma \sim \sigma_0^{1/3}$ quickly and then gradually accelerate as $\Gamma \propto R^{1/3}$ until reaching $\Gamma \sim \sigma_0$ (Granot et al. 2011), where $\sigma_0 \equiv \frac{B_0^2}{8\pi\rho_c c^2}$ is the initial magnetization parameter at the base of the flow, ρ_c is the density of the flux rope in the corona, and B_c is the magnetic field in the corona near the flux rope region. Unfortunately, both B_c and especially ρ_c are poorly constrained by current analytical theory and numerical simulations of accretion flows. MHD numerical simulations of both optically thin ADAFs and standard thin disks show that the density in the corona is strongly inhomogeneous and stratified. A density contrast as large as ~ 5 orders of magnitude has been achieved in numerical simulations (Hirose, Krolik & Blaes 2009), which can be regarded as a lower limit due to the “density floor” imposed in the simulations by hand to stabilize the simulations. Given the uncertainties, we estimate the density of corona by analogy with the case of the Sun. The density at the bottom of the solar corona is about $7 \sim 12$ orders of magnitude lower than the density of the turbulence layer of the Sun (counterpart of the accretion disk main body). We then adopt a fiducial value for the density ratio between the disk and the flux rope $\rho/\rho_c \sim 10^9$. The magnetic field strength in the corona (B_c) is not so different from that in the disk. Here we assume that the magnetic field energy density in the flux rope is 10 times weaker than that in

³ The power output from the innermost NDAF region with $10 > r > 3$ can become comparable to that from the outer ADAF. However, the blobs emitted from these regions are closely packed, which would likely collide below the photosphere and would not give rise to significant variability. In addition, this power can be consumed to penetrate the star and open a funnel for blobs ejected later from the ADAF region.

the accretion flow. We then have

$$\sigma_0 \approx 3500 \left(\frac{\rho/\rho_c}{10^9} \right) \beta_{-1} \left(\frac{r}{200} \right)^{-1}. \quad (22)$$

For a higher β value as discussed above, a smaller density contrast can be incorporated to achieve the same σ_0 value. The Lorentz factor of the outflow in the emission region is $\Gamma \leq \sigma_0$ depending on the radius of the emission region, R_{GRB} , from the central engine. Because of the inhomogeneity of the density of the corona, the value of σ_0 is expected to be variable for different blobs. This implies that their collisions will be efficient.

The initial size of each blob is of order the size of the disk, i.e. $\Delta_0 \sim R_{\text{disk}} \sim 2 \times 10^8 \text{ cm } M_3(r/200)$. The blob is initially at rest, and is accelerated by magnetic pressure gradient. First it undergoes a non-relativistic phase (Yuan et al. 2009), during which the bubble continues to expand adiabatically. This phase lasts for a time scale of reconnection near the base of the flux rope, i.e. $t_{\text{rec}} \sim R_{\text{disk}}/v_{\text{rec}} \sim 0.7 \text{ s } (r/200)(0.01c/v_{\text{rec}})$. The expansion speed is essentially $\sim c$ for a high- σ bubble. So the size of the bubble grows to $\Delta \sim ct_{\text{rec}} \sim 2 \times 10^{10} \text{ cm}$ before entering the relativistic phase, during which the lab-frame width essentially stops growing.

During the relativistic phase, the Lorentz factor at the distance $R_0 \sim \Delta$ is $\Gamma(R_0) \sim \sigma_0^{1/3} \sim 15 (10^9 \rho/\rho_c)^{1/3} \beta_{-1}^{1/3} (r/200)^{-1/3}$. With a slow increase $\Gamma \propto R^{1/3}$ (Granot et al. 2011), one would reach the full Lorentz factor $\Gamma_{\text{full}} = 3500$ at a radius $R_{\text{full}} \sim 3.8 \times 10^{17} \text{ cm}$. GRB prompt emission likely occurs at much smaller radii where $\Gamma(R_{\text{GRB}}) \ll \sigma_0$. A plausible scenario would be the Internal Collision-induced MAgnetic Reconnection and Turbulence (ICMART) scenario conjectured by (Zhang & Yan 2011). Within this scenario, most magnetic energy is discharged in the ICMART region, so that after dissipation σ drops to around or below unity, and the final bulk Lorentz factor $\Gamma \sim \Gamma(R_{\text{GRB}}) \ll \sigma_0$. For example, for $R_{\text{GRB}} \sim 10^{15} \text{ cm}$, $\Gamma_{\text{GRB}} \sim 550$ for $\sigma_0 = 3500$, and $\Gamma_{\text{GRB}} \sim 260$ for $\sigma_0 = 350$.

The trigger of ICMART events is through internal collisions. It is expected that σ_0 of the blobs may vary from case to case due to the fluctuation of ρ_c and B_c . The later ejected faster blobs would inevitably catch up with the preceding slower ones. Such collisions of magnetic blobs have been frequently observed in the Sun (Gopalswamy et al. 2002), and are often invoked to explain the bright knots or flares commonly observed in other astrophysical systems such as AGN jets and Crab nebula. The separation between the blobs is $d \sim ct_{\text{int}} \sim 10^{11} \text{ cm}$. The typical collision radius is

$$R_{\text{GRB}} \sim \Gamma^2 ct_{\text{int}} = 10^{15} \left(\frac{\Gamma}{100} \right)^2 \beta_{-1}^{-0.5} M_3 \left(\frac{r}{200} \right)^{1.5} \text{ cm}. \quad (23)$$

For a typical GRB $\Gamma \geq 100$ (Lithwick & Sari 2001; Liang et al. 2010), this radius is consistent with various observational constraints that suggest a relative large R_{GRB} (Kumar et al. 2006; Nishikori et al. 2006; Zhang & Pe'er 2009; Shen & Zhang 2009; Fan 2010).

The polarities of the magnetic field lines trapping the two colliding blobs are in general opposite or have some large angles. This greatly eases the trigger of ICMART events. The initial fast reconnection would induce turbulence and a cascade of turbulent reconnection (Zhang & Yan 2011; Lazarian & Vishniac 1999). A large fraction of the magnetic energy stored in the blobs would be efficiently con-

verted into lepton energy and then into photon energy, giving rise to radiatively efficient GRB emission (Zhang & Yan 2011; Uzdensky & McKinney 2011). The model can also account for the two variability components as observed in GRBs (Gao, Zhang, & Zhang 2012; Vetere et al. 2006): the angular spreading time (Piran 1999)

$$t_{\text{ang}} \sim \frac{R_{\text{GRB}}}{c\Gamma^2} \sim t_{\text{int}} \sim 3.4 \beta_{-1}^{-0.5} M_3 \left(\frac{r}{200} \right)^{1.5} \text{ s}. \quad (24)$$

corresponds to the time scale of the slow component, while the fast variability is related to relativistic turbulence (Narayan & Kumar 2009).

4. SUMMARY AND DISCUSSION

Observations to relatively well-studied black hole systems such as AGNs and black hole X-ray binaries show the existence of two types of jets, namely continuous and episodic ones. GRB observational data require that the central engine launches a magnetically dominated episodic jet. The traditional BZ jet model requires that the accretion rate is highly variable or that a continuous jet is disrupted by instabilities during propagation. In this paper we propose an intrinsically episodic central engine model for GRBs by invoking ejections of episodic magnetic blobs from a hyper-accretion flow around a black hole. Our basic calculations suggest that the predicted energetics and timescales are consistent with the observations. More detailed numerical simulations are called for to validate the scenario.

This model has several appealing features. Firstly, the episodic jets invoked in our model have obtained strong observational supports in other black hole systems (e.g., Yuan et al. 2009, and references therein). Observations show that they are more powerful than continuous jets. Secondly, this model naturally satisfies the observational requirement for the lack of a bright photosphere component in the GRB spectra (Zhang & Pe'er 2009), since the engine naturally launches a magnetized outflow. Thirdly, episodic jets intrinsically consist of individual blobs, whose collisions are naturally expected. These collisions are an important ingredient to interpret GRB variability within the magnetically dominated model (Zhang & Yan 2011). Fourthly, the directions of the magnetic fields surrounding the two adjacent blobs in general have some angles. This greatly eases triggering fast reconnection and the subsequent turbulence, which can efficiently convert magnetic energy into radiation (Zhang & Yan 2011; Lazarian & Vishniac 1999; McKinney & Uzdensky 2011).

We add two notes here. First, we did not discuss collimation of episodic jets in the progenitor stellar envelope. We point out that the same physics invoked in the magnetic tower model (Uzdensky & MacFadyen 2006) should equally apply to our model. Second, the scenario we propose should also work for a neutron star, not necessarily a black hole, as has been discussed by some previous authors (e.g. Blackman et al. 1996; Kluzniak & Ruderman 1998; Dai et al. 2006; Metzger et al. 2011).

It may be difficult to differentiate this model from other GRB central engine models from the GRB observational data. Due to their large distances and small scales, it is essentially impossible to witness ejection of magnetic blobs from GRBs. Nonetheless, observing episodic blobs may be possible for nearby AGNs and X-ray binaries with high spatial and temporal resolution observations in the future. These observations may be used to verify this generic episodic central engine model.

We thank Ramesh Narayan, Tsvi Piran, and Rongfeng Shen for valuable discussions and the referee for useful comments. FY is supported by the NSFC (grants 10825314, 10833002, 11121062, and 11133005), the National Basic

Research Program of China (973 Program 2009CB824800), and the CAS/SAFEA International Partnership Program for Creative Research Teams. BZ is supported by National Science Foundation (grant AST-0908362) and NASA (grant NNX10AD48G).

REFERENCES

- Abdo, A. A. et al. 2009, *Science*, 323, 1688
 Balbus S. A., & Hawley J. F., 1991, *ApJ*, 376, 214
 Balbus S. A., & Hawley J. F., 1998, *Rev. Mod. Phys.*, 70, 1
 Band, D. et al. 1993, *ApJ*, 413, 281
 Beloborodov, A. 2003, *ApJ*, 588, 931
 Blackman, E. G., Penna, R. F. & Varnière, P. 2008, *NewA*, 13, 244
 Blackman, E. G., Yi, I. & Field, G. B. 1996, *ApJ*, 473, L79
 Blandford, R. D. & Znajek, R. L. 1977, *MNRAS*, 179, 433
 Chatterjee, R. et al. 2009, *ApJ*, 704, 1689
 Chen, W., & Beloborodov, A., 2007, *ApJ*, 657, 383
 Dai, Z. G. et al., 2006, *Science*, 311, 1127
 Dai, Z. G. & Lu, T. 1998, *PhRvL*, 81, 4301
 Doi, A. et al. 2011, arXiv:1106.2930
 Fan, Y. Z. 2010, *MNRAS*, 403, 483
 Fender, R., & Belloni, T. M., 2004, *ARA&A*, 42, 317
 Fishman, G. J. & Meegan, C. A. 1995, *ARA&A*, 33, 415
 Frail, D. et al., 2001, *ApJ*, 562, L55
 Gao, H., Zhang, B.-B., Zhang, B. 2012, *ApJ*, 748, 134
 Granot, J. et al., 2011, *MNRAS*, 411, 1323
 Gopalswamy, N. et al., 2002, *ApJ*, 572, L103
 Hakkila, J. et al. 2003, *ApJ*, 582, 320
 Hawley, J. F., Guan, X. & Krolik, J. H. 2011, *ApJ*, 738, 84
 Hirose, S., Krolik, J. & Blaes, O. 2009, *ApJ*, 691, 16
 Hjellming, R. M. & Rupen, M. P. 1995, *Nat*, 375, 464
 Horiuchi et al., 1998, *PASJ*, 40, 147
 Johansen, A. & Levin, Y. 2008, *A&A*, 490, 501
 Kluzniak, W. & Ruderman, M. 1998, *ApJ*, 505, L113
 Kudoh, T., Matsumoto, R. & Shibata, K. 2002, *PASJ*, 54, 267
 Kumar, P. et al., 2006, *MNRAS*, 367, L52
 Lazarian, A., & Vishniac, E. T., 1999, *ApJ*, 517, 700
 Li, L.-X. 2000, *ApJ*, 531, L111
 Liang, E.-W., et al., 2008, *ApJ*, 675, 528
 Liang, E.-W., et al., 2010, *ApJ*, 725, 2209
 Lin, J. et al., 1998, *ApJ*, 504, 1006
 Lithwick, Y. & Sari, R. 2001, *ApJ*, 555, 540
 Lynden-Bell, D. 1996, *MNRAS*, 279, 389
 Machida, M., Nakamura, K. & Matsumoto, R. 2004, *PASJ*, 56, 671
 MacFadyen, A. I. & Woosley, S. E. 1999, *ApJ*, 524, 262
 Marscher, A. P. et al. 2002, *Nat*, 417, 625
 Mészáros, P., Rees, M. J., & Wijers, R. A. M. J., 1999, *New Astron.*, 4, 303
 Mészáros, P. & Rees, M. J., 2000, *ApJ*, 530, 292
 Metzger, B. D. et al. 2011, *MNRAS*, 413, 2031
 McKinney, J. C. & Uzdensky, D. 2012, *MNRAS*, 419, 573
 Mirabel, I. F., Rodriguez, L. F. 1994, *Nature*, 371, 46
 Mizuno, Y., Lyubarsky, Y., Nishikawa, K.-I., Hardee, P. E. 2009, *ApJ*, 700, 684
 Morsony, B. J., Lazzati, D., Begelman, M. C. 2010, *ApJ*, 723, 267
 Narayan, R. & Kumar, P. 2009, *MNRAS*, 394, L117
 Narayan, R., Paczynski, B., & Piran, T., 1992, *ApJ*, 395, L83
 Narayan, R., Piran, T., & Kumar, P. 2001, *ApJ*, 557, 949
 Nishikori, H., Machida, M., & Matsumoto, R. 2006, *ApJ*, 641, 862
 Norris, J. et al. 1996, *ApJ*, 459, 393;
 Paczyński, B. 1986, *ApJ*, 308, L43
 Pe'er, A. et al. 2006, *ApJ*, 642, 995
 Piran, T., 1999, *Phys. Rep.*, 314, 575
 Racusin, J. et al., 2009, *ApJ*, 698, 43
 Romanova et al. 1998, *ApJ*, 500, 703
 Shen, R.-F., & Zhang, B. 2009, *MNRAS*, 398, 1936
 Shibata, K., Tajima, T. & Matsumoto, R. 1990, *ApJ*, 350, 295
 Sorathia, K. A., Reynolds, C. S., Stone, J. M., & Beckwith, K. 2012, *ApJ*, 749, 189
 Tchekhovskoy, A., Narayan, R., & McKinney, M. C. 2010, *New Astron.*, 15, 749
 Uzdensky, D. A. & MacFadyen, A. I. 2006, *ApJ*, 647, 1192
 Uzdensky, D. A. & MacFadyen, A. I. 2007, *ApJ*, 669, 546
 Uzdensky, D. A. & McKinney, J. C. 2011, *Physics of Plasmas*, 18, 042105
 Vetere, L. et al. 2006, *A&A*, 447, 499
 Wang, X. Y. & Mészáros, P. 2007, *ApJ*, 670, 1247
 Yuan, F. 2011, *ASP Conf. Ser.* 439, (ed. Mark R. Morris, Q. Daniel Wang, and Feng Yuan), 346
 Yuan, F., Lin, J., Wu, K., & Ho, L. 2009, *MNRAS*, 395, 2183
 Zhang, B. & Pe'er, A. 2009, *ApJ*, 700, L65
 Zhang, B. & Yan, H. 2011, *ApJ*, 726, 90
 Zhang, B.-B. et al. 2011, *ApJ*, 730, 141
 Zhang, W., Woosley, S. E., MacFadyen, A. I. 2003, *ApJ*, 586, 356